

# Directional Shear Force Microscopy

A. R. Burns\* and R. W. Carpick<sup>†</sup>  
*Sandia National Laboratories, MS 1413*  
*Albuquerque, NM 87185-1413*

## Abstract

We describe a new technique, based on shear force microscopy, that allows one to detect shear forces in a chosen direction at the nanometer scale. The lateral direction of an oscillating probe tip is determined by selecting which of the four quadrants are excited on the piezo driver. The shear forces depend directly on this lateral direction if structural anisotropies are present, as confirmed with polydiacetylene monolayers.

\* Corresponding author: aburns@sandia.gov, (505)-844-9642, FAX (505)-844-5470

† Current address: Department of Engineering Physics, University of Wisconsin-Madison, 1500 Engineering Dr., Madison, WI 53706-1687.

## **DISCLAIMER**

This report was prepared as an account of work sponsored by an agency of the United States Government. Neither the United States Government nor any agency thereof, nor any of their employees, make any warranty, express or implied, or assumes any legal liability or responsibility for the accuracy, completeness, or usefulness of any information, apparatus, product, or process disclosed, or represents that its use would not infringe privately owned rights. Reference herein to any specific commercial product, process, or service by trade name, trademark, manufacturer, or otherwise does not necessarily constitute or imply its endorsement, recommendation, or favoring by the United States Government or any agency thereof. The views and opinions of authors expressed herein do not necessarily state or reflect those of the United States Government or any agency thereof.

## **DISCLAIMER**

**Portions of this document may be illegible  
in electronic image products. Images are  
produced from the best available original  
document.**

The dependence of friction upon sliding direction arises from structural properties of the materials in contact. For example, friction anisotropy was correlated with the relative crystallographic orientation of the sliding interfaces with a surface forces apparatus[1] and with an atomic force microscope (AFM)[2]. It has also been observed with AFM friction or "lateral" force imaging of highly-ordered Langmuir-Blodgett films[3,4]. Scanning probe friction anisotropy can reveal specific structural properties which may not be seen in topographic images. Such experiments can then elucidate how friction is fundamentally related to these structural properties.

In AFM, the "lateral" force signal is usually acquired by monitoring the amount of twisting induced on the cantilever by the friction or shear force of the sliding contact between the tip and the sample [5,6]. Since the twisting is maximized when the scan direction is perpendicular to the axis of the cantilever, and is absent when the scan is parallel to the axis, meaningful lateral force measurements are constrained to the perpendicular scan direction. Thus, to measure friction as a function of angle, a cumbersome sample rotation procedure is required. An alternate method for detecting shear forces was introduced with optical fiber-based near field scanning optical microscopes[7,8], which required a sensitive feedback signal for distance regulation. The shear forces experienced at the tip of the laterally oscillating fiber have been shown to be an effective way to study fundamental aspects of friction[9,10]. In this letter, we show that by virtue of the lateral orientation of the oscillating fiber, *directional* shear force microscopy can be used to reveal friction anisotropy, independent of scan direction.

The directional shear force experiment is shown schematically in Fig. 1. An optical fiber is mounted concentrically with respect to the four quadrant "dither" piezo (Stavely EBL#1, 0.125 inch diameter, 0.18 inch long) by gluing it inside a short 24-gauge stainless tube that is held by a metal clip (not shown) in a ceramic cap on the piezo[11]. The end of the optical fiber is HF-etched to form a  $200 \mu\text{m}$  conical taper with a parabolic tip radius of approximately 50 nm[12]. The optical fiber has mechanical resonances in the 12-30 kHz range for fiber lengths of about 1.5 mm protruding from the metal tube, and a  $Q$  of 60-90 before contact. The lateral motion amplitude of the fiber is determined by  $A_{\text{piezo}}Q$ , where  $A_{\text{piezo}}$  is the piezo drive amplitude. The piezo is driven by

RECEIVED  
OCT 11 2000  
OSTI

a sinusoidal voltage (1.23 nm/V) applied to two adjacent quadrants (*e.g.*, +y,-x in Fig. 1), and fiber motion is detected by phase-sensitive lock-in amplified voltages induced on the other two quadrants (in this case, +x,-y). Details and variations on this very sensitive technique have been published elsewhere[10,11,13,14]. We use a sinusoidal drive voltage of  $\pm 10$  mV with respect to the grounded inner electrode, which results in a tip lateral motion amplitude of  $A_{\text{piezo}}Q \approx 1$  nm for  $Q = 80$ . The unique aspect of this technique is that the direction of the lateral motion can be changed by switching to new drive and detection quadrants. Thus we can change the direction by  $90^\circ$  by switching to +y,+x drive quadrants (detect with -x,-y). This was verified by CCD imaging of the moving tip under 800X magnification (and drive amplitude of  $\pm 40$  V).

A typical frequency response of the fiber-piezo system (+y,+x drive) is shown in Fig. 2. The piezoelectric signal (lower), detected with the -y,-x quadrants, is compared with the lock-in detected signal of laser light scattered off the fiber tip (upper). The laser is used as an initial check to determine which peaks are true fiber resonances. The angle of the laser beam is oriented at  $45^\circ$  with respect to both drive directions (see Fig. 1) to insure equal signal strength when the drive direction is switched. Ideally, the mechanical resonance of the fiber should have one mode with a frequency independent of drive direction. However, due to the slight asymmetries in the way the optical fiber is mounted, multiple modes appear and there are significant shifts ( $\sim 1$  kHz) in the resonance frequencies when the drive direction is changed. Some of the modes are circular or elliptical, but these can be avoided by selecting those that have the strongest optical scattering signal. The strongest features usually have equal ( $\pm 5\%$ ) signal amplitudes for each drive direction, both in the piezoelectric signals and the optical signals.

One can see that the piezoelectric signals at the tip resonances have a dispersive appearance. As noted previously by Brunner *et al.*[14], this effect is most likely due to the interference of the tip resonance signal with the background signal coming from the drive piezo. We can model that as follows. The equation of motion for a damped harmonic oscillator can be given by:

$$\ddot{x} + 2\beta\dot{x} + \omega_0^2 = A \cos \omega t \quad (1)$$

where  $x$  is the displacement at frequency  $\omega$ ,  $\beta$  is the damping term,  $A$  is the driving force, and  $\omega_0$  is the resonance frequency. A possible solution to Eq. 1 is:

$$x(t) = D \cos(\omega t - \theta) \quad (2)$$

where  $\theta$  is the phase shift of  $x$  with respect to  $A$ , and  $D$  is the amplitude of  $x$ . By substituting Eq. 2 into Eq. 1, it can be shown that:

$$\cos \theta = \frac{\omega_0^2 - \omega^2}{\sqrt{(\omega_0^2 - \omega^2)^2 + 4\omega^2\beta^2}} \quad (3)$$

$$D = \frac{A}{\sqrt{(\omega_0^2 - \omega^2)^2 + 4\omega^2\beta^2}} \quad (4)$$

If there are no other mechanical resonances in the frequency region except that of the fiber, the amplitude  $D$  (Eq. 4) of the fiber interferes at a phase shift  $\theta$  with the constant background (normally subtracted by the lock-in) of the drive piezo, thus the detected amplitude  $D_{det}$  is given by:

$$D_{det} \approx D \cos \theta = \frac{(\omega_0^2 - \omega^2)A}{(\omega_0^2 - \omega^2)^2 + 4\omega^2\beta^2} \quad (5)$$

We see in the inset of Fig. 2 that Eq. 5 fits the data fairly well with  $\omega_0 = 13.936$  kHz and  $\beta = 1050$ . Also,  $Q \equiv (\omega_0/2\beta) = 66$ , which is consistent with other measurements, including a fit of the optical signals with Eq. 4. To use this signal for shear-force feedback, we sit on the positive-going peak and feedback on a 10% attenuation. For a  $\pm 10$  mV drive,  $A_{piezo} \cong 0.01$  nm, and we estimate from Ref. [10] that the shear force  $F$  at 10% attenuation is  $F \cong A_{piezo} k(0.10) = 0.15$  nN, where  $k = 150$  N/m is the spring constant of the glass fiber.

In Fig. 3, we demonstrate the directional shear-force technique. We use a Langmuir-Blodgett monolayer of the conjugated polymer polydiacetylene (PDA) that has been transferred to an

atomically-flat  $\text{SiO}_2$  substrate[15]. AFM measurements showed that the PDA exhibits friction anisotropy that correlates with the direction of its polymer backbones that run parallel to the surface in domains ( $>100 \mu\text{m}^2$ ) with different in-plane orientations[4]. Details concerning the structure of these films are reported elsewhere [4,15], but for the present purpose we note that the AFM friction force is highest (lowest) when scanning perpendicular (parallel) to the backbone direction. In Fig. 3, we first collect an image A ( $3.0 \times 2.4 \mu\text{m}^2$ ) using the  $+y, -x$  drive direction at  $\pm 10 \text{ mV}$  excitation (14.725 kHz resonance) as our shear force signal. The lateral  $+y, -x$  drive direction relative to the  $0^\circ$  scan angle is indicated by the arrow. Two contrasting domains can be clearly seen. The brightest regions are those where the tip experienced the highest shear forces, due to a larger perpendicular component of the backbone direction relative to the lateral drive direction. We now acquire another image (B) under identical conditions at a scan angle of  $90^\circ$ . We see that the image has rotated  $90^\circ$ , but is otherwise unchanged. *Thus the shear-force signal is not dependent on scan direction.* We now raise the tip out of contact, switch to the  $+y, +x$  drive direction, tune it to the appropriate resonance (13.936 kHz), and bring the tip back into contact under 10% damped feedback. The  $0^\circ$  scan angle image C has reversed contrast relative to A and B. *This contrast can only be due to shear forces because the topology is unchanged.* We repeat the scan under  $90^\circ$  scan angle to acquire image D which has, again, only rotated the image relative to C.

In order to reveal structural friction anisotropy via directional shear forces, adhesion must be reduced as much as possible. Adhesion from isotropic chemical forces is expected to reduce contrast due to structural anisotropy. For this reason, all of the data was acquired with a hydrophobic glass tip that was coated with a monolayer of  $\text{CF}_3(\text{CF}_2)_5(\text{CH}_2)_2\text{-SiCl}_2$  via vapor phase deposition[16]. Water layers are expected to be present under the ambient conditions of  $\sim 20\%$  relative humidity. However, there was no evidence of capillary condensation between the tip and the PDA films. Thus the shear force contrast that we see is due to structural aspects of the PDA monolayer, with negligible contributions from chemical forces[10,17].

In shear-force feedback microscopy, contrast is derived through height, friction (as in Fig. 3), or both. For this reason, “topographs” derived from shear-force feedback, as commonly used in

near-field microscopy, should be used with caution. One way to distinguish height from friction in the absence of significant adhesion is to change the direction of the lateral motion. Images of the same PDA sample that show both friction contrast reversal and apparent topology are shown in Fig. 4 (all  $2.4 \times 2.4 \mu\text{m}^2$ ). Here the top two images taken at the orthogonal lateral directions are very similar with various defects in the film (*e.g.*, black holes), except for the small domain in the lower right corner. In image A it appears lower, whereas in B it appears higher than the surrounding area. This contrast reversal must be due to the anisotropy in shear forces for that domain. In the lower images C and D, where the bright (high) regions are  $\sim 70 \text{ \AA}$  bilayers of PDA, we see that true topography is not affected by the direction of lateral motion.

We have demonstrated that directional shear force microscopy can reveal friction anisotropy independent of scan direction and is thus an excellent tool for nanoscale tribology. Refinements to the fiber mounting should reduce the fiber resonance to one mode with a frequency independent of drive direction. Other refinements will include electronics that provide continuously variable direction control. Simultaneous normal force sensing has also been demonstrated[9,10]. We acknowledge help from S. Stranick concerning tip mounting and B. Swartzentruber for electronics. R.W.C. acknowledges the support of the Natural Sciences and Engineering Research Council of Canada. Sandia is a multiprogram laboratory operated by Sandia Corporation, a Lockheed Martin Company, for the United States Department of Energy under Contract DE-AC04-94AL85000.

## References

- [1] M. Hirano, K. Shinjo, R. Kaneko, and Y. Murata, *Phys. Rev. Lett.* **67**, 2642 (1991).
- [2] P. E. Sheehan and C. M. Lieber, *Science* **272**, 1158 (1996).
- [3] M. Liley, D. Gourdon, D. Stamou, U. Meseth, T. M. Fischer, C. Lautz, H. Stahlberg, H. Vogel, N. A. Burnham, and C. Duschl, *Science* **280**, 273-5 (1998).
- [4] R. W. Carpick, D. Y. Sasaki, and A. R. Burns, *Trib. Lett.* **7**, 79 (1999).
- [5] G. Meyer and N. Amer, *Appl. Phys. Lett.* **57**, 2089 (1990).
- [6] S. Alexander, L. Hellemans, O. Marti, J. Schneir, V. Elings, P. K. Hansma, M. Longmire, and J. Gurley, *J. Appl. Phys.* **65**, 164 (1989).
- [7] E. Betzig, P. L. Finn, and J. S. Weiner, *Appl. Phys. Lett.* **60**, 2484 (1992).
- [8] R. Toledo-Crow, P. C. Yang, Y. Chen, and M. Vaez-Iravani, *Appl. Phys. Lett.* **60**, 2957 (1992).
- [9] A. R. Burns, J. E. Houston, R. W. Carpick, and T. A. Michalske, *Phys. Rev. Lett.* **82**, 1181 (1999).
- [10] A. R. Burns, J. E. Houston, R. W. Carpick, and T. A. Michalske, *Langmuir* **15**, 2922 (1999).
- [11] S. J. Stranick, L. J. Richter, and R. R. Cavanagh, *J. Vac. Sci. Technol. B* **16**, 1948 (1998).
- [12] P. Hoffmann, B. Dutoit, and R.-P. Salathe, *Ultramicroscopy* **61**, 165 (1995).
- [13] J. Barentz, O. Hollricher, and O. Marti, *Rev. Sci. Instrum.* **67**, 1912 (1996).
- [14] R. Brunner, A. Bietsch, O. Hollricher, and O. Marti, *Rev. Sci. Instrum.* **68**, 1769 (1997).
- [15] D. Y. Sasaki, R. W. Carpick, and A. R. Burns, *J. Colloid Interface Sci.* **in press** (2000).
- [16] T. M. Mayer, M. P. d. Boer, N. D. Shinn, P. J. Clews, and T. A. Michalske, *J. Vac. Sci. Technol. B* **in press** (2000).
- [17] C. D. Frisbie, L. F. Rozsnyai, A. Noy, M. S. Wrighton, and C. M. Lieber, *Science* **265**, 2071 (1994).

## Figure Captions

Fig. 1: Schematic of directional shear-force experiment. An optical fiber is mounted concentrically in a four-quadrant piezo tube. The lateral motion of the fiber in one direction (solid arrows) is caused by applying drive voltages to two adjacent quadrants, *e.g.*, the +y,-x pair; motion orthogonal to this direction is produced by switching the drive to the +y,+x pair. A laser beam (dotted line) detects motion for either direction and is used only to identify tip resonances. At the bottom of the figure, CCD images are shown for the two drive directions.

Fig. 2: Frequency response of tip lateral motion for drive voltages applied to +y,+x quadrants. (A) As detected optically by laser light scattering. (B) As detected piezoelectrically with quadrants (-y,-x). The large optical peak at left identifies the lateral (linear) motion mode. Because the optical signals are much weaker relative to the piezoelectric signals, this data was taken with a drive amplitude of  $\pm 56$  mV. (Inset) Normalized frequency response data (open circles) from piezoelectric signal over smaller frequency (kHz) range, and compared to theory (solid line) discussed in text.

Fig. 3: Directional shear force images ( $3.0 \times 2.4 \mu\text{m}^2$ ) of one region of a PDA monolayer. (A) With +y,-x drive (direction shown at top with respect to image) and  $0^\circ$  scan angle. (B) Same as (A), except  $90^\circ$  scan angle. (C) With +y,+x drive (direction shown at top with respect to image) and  $0^\circ$  scan angle. (D) Same as (C), except  $90^\circ$  scan angle.

Fig. 4: Directional shear force images (all  $2.4 \times 2.4 \mu\text{m}^2$ ,  $0^\circ$  scan angle) of two regions of a PDA film. (A) First region with +y,-x drive (direction shown at top with respect to image). (B) Same region, except with +y,+x drive (direction shown at top with respect to image). (C) Second region showing  $70 \text{ \AA}$  bilayer (bright areas) taken with +y,-x drive direction. (D) Same region, except with +y,+x drive direction.

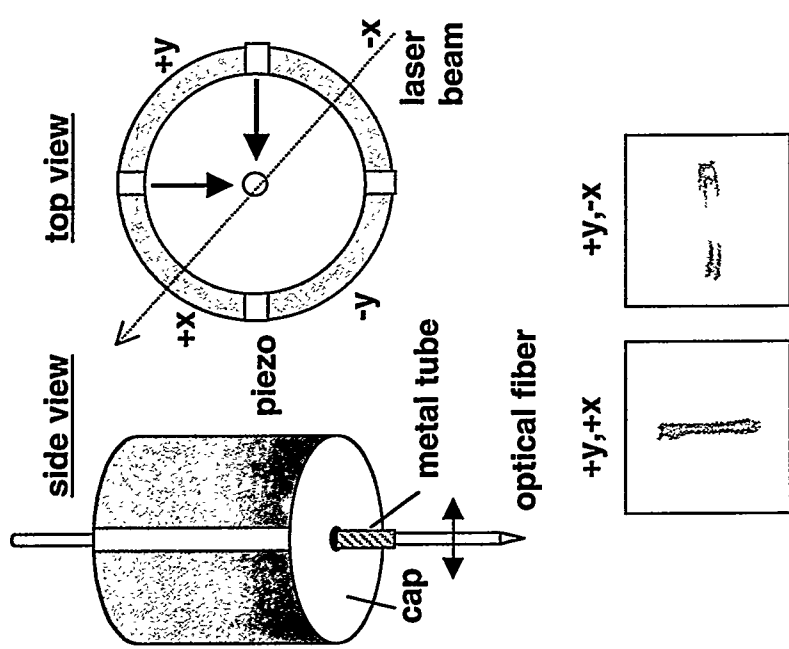


Fig. 1, Burns *et al.*

Fig. 2, Burns *et al.*

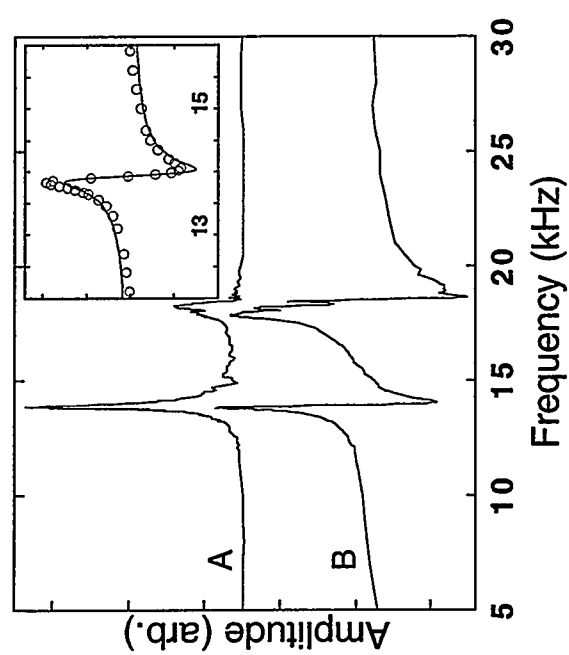


Fig. 3, Burns *et al.*

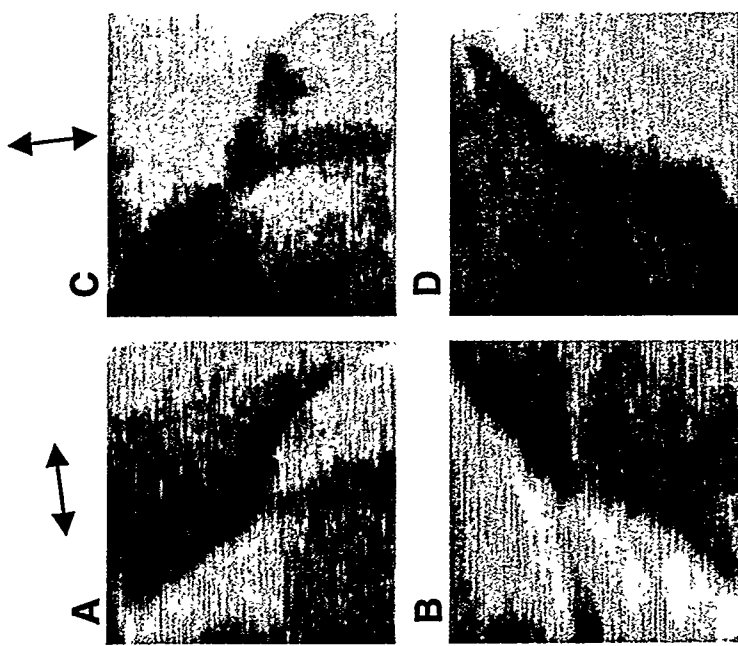


Fig. 4, Burns *et al.*

